REQUIREMENTS FOR A BEAM SWEEPING SYSTEM FOR THE FERMILAB ANTIPROTON SOURCE TARGET*

F. M. Bieniosek, K. Anderson and K. Fullett
Fermilab, P.O. Box 500, Batavia, IL 60510 USA

Abstract

In order to increase the rate of production of antiprotons, intensity of the incident 120-GeV proton beam on target is scheduled to increase to 5×10^{12} protons per pulse. Intensity in the range of 3×10^{12} has already been sufficient to damage the nickel antiproton production target. To continue to operate with a tightly-focused primary beam spot on the target, and thus maintain yield, we plan to spread the hot spot on target with a beam sweeping system. Operation of the system will require a deflection of the beam with pairs of 625-kHz magnets upstream and downstream of the target. We are investigating both ferrite and laminated-iron magnet designs for operation in the harsh environment downstream of the target.

HIGH-INTENSITY TARGETRY

Antiprotons are collected from the interaction of a 120-GeV proton beam with a solid nickel target. The efficiency of collecting antiprotons from the target rises as the size of the proton beam spot on the target is reduced. However at the same time the peak energy deposition on target rises. Under Main Injector conditions (5×10^{12} protons in a 1.6-μs pulse), the spot size will have to be increased to at least 0.25 mm to keep peak energy deposition near current levels. To bring the density of energy deposition with a 0.1-mm spot size down to currently-existing levels, a system to sweep the beam spot on the target has been proposed.[1]

Measurements of yield with beam spot position on the target [2] show a Gaussian shape in both horizontal and vertical dimensions, where $\sigma_x = 0.48$ mm, and $\sigma_y = 0.65$ mm. The shape of the yield distribution is determined by the acceptance and lattice functions of the Debuncher and the AP2 beam line. If the incoming proton beam is itself a Gaussian, $\sqrt{2/\pi}\,\sigma_{bx}^{-1}\exp\left(-x^2/2\sigma_{bx}^2\right)$ in both planes, with characteristic spot size σ_{bx} and σ_{by}, then the dependence of the yield on spot size, normalized to the yield for an infinitesimal point beam, becomes

$$Y = \frac{\sigma_x \sigma_y}{\sqrt{\sigma_x^2 + \sigma_{b_x}^2}\,\sqrt{\sigma_y^2 + \sigma_{b_y}^2}}. \qquad (1)$$

This curve is plotted in Fig. 1 for a circular beam spot. Also shown are MARS10 calculations of energy deposition in a copper target as a function of beam size for $N=5\times10^{12}$ protons per pulse.[3] A small fraction (typically less than 10%) of the deposited energy is released as a stress wave by the elastic properties of the metal; the remainder is deposited locally for a time much longer than a beam pulse. The spot size under current operating conditions is about σ_{bx}=0.15 mm; σ_{by}= 0.23 mm. Estimates of the peak instantaneous energy deposition for the highest intensity achieved to date (3.4×10^{12}) indicate an energy deposition of about 800 J/g. This is above the melting point of copper (about 600 J/g), and close to the melting point of nickel (about 1000 J/g). Local disintegration of the target has been observed when the target rotation mechanism failed. The damage was presumably caused by the integrated radiation dosage to the affected spot, combined with severe repetitive thermal and mechanical stress. Less severe damage was observed with a slowly-rotating target.[4] In order to maintain peak energy deposition below present levels after the Main Injector begins operation, it will be necessary to increase the spot size. The alternative is to sweep the beam on the target, and reduce the spot size to the smallest attainable, leading to a 15-20% increase in yield. As incident beam intensity continues to rise, beam sweeping will become increasingly important to operation of the Antiproton Source.

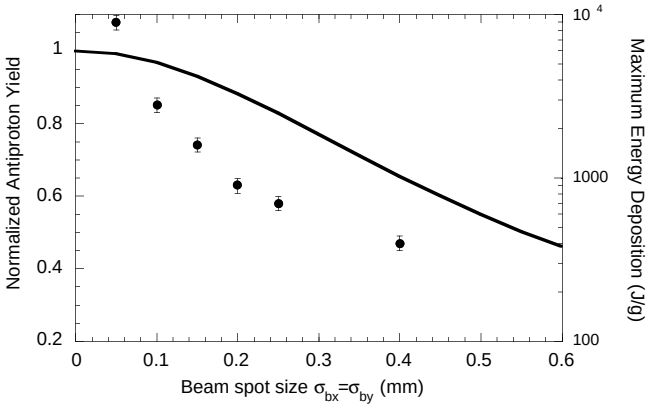

Figure 1. Scaling of yield (curve) and peak energy deposition (points) in the target as a function of beam spot size. The values for energy deposition were taken from Ref. 3.

The effective size of the energy deposition profile is comparable to or larger than the beam spot size. For a circular Gaussian energy deposition profile with variance σ in both planes, swept in a circle of radius r_0, the radial energy deposition profile is

$$E(r) = \exp\left[-\frac{r^2 + r_0^2}{2\sigma^2}\right] I_0\left(\frac{r\,r_0}{\sigma^2}\right), \qquad (2)$$

where I_0 is the modified Bessel function. The peak of the energy deposition curve (Eq. 2) is shown in Fig. 2 as a function of the ratio of sweep radius to σ. Increasing amplitude of beam sweep rapidly reduces peak energy

deposition for r_0 / σ near 2. The effect is that a sweeep radius of 0.33 mm reduces the peak energy deposition to about 600 J/g for 5×10^{12} protons per pulse[3]. This level of energy deposition is likely to be acceptable for reliable operation in nickel targets.

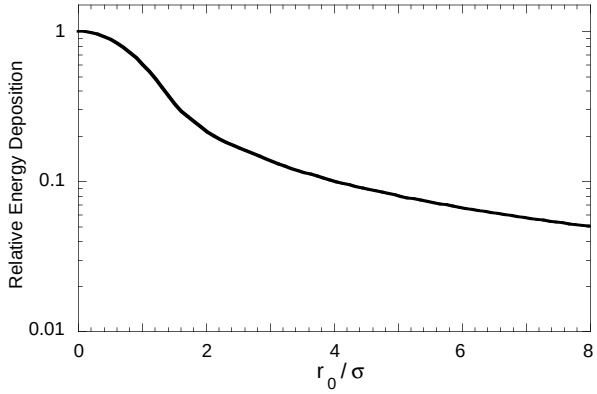

Figure 2. Effect of beam sweeping on the maximum local energy deposition for an initially Gaussian energy deposition.

SWEEPING SYSTEM

The beam sweeping scheme utilizes two upstream sweep magnets driven in quadrature by a 625-kHz sinusoidal current waveform to trace a circular pattern on the target with the 120-GeV proton beam, followed by two downstream magnets to redirect the 8-GeV antiprotons exiting the collection lens parallel to the AP2 transport line[5]. Figure 3 shows a layout of the target station with sweeping system installed. The AP1 beamline transports and focuses the 120-GeV protons from the Main Ring onto the target. Antiprotons created in the target are collected by a lithium lens, and deflected by the pulsed magnet into the AP2 beam line for injection into the Debuncher. The upstream sweep magnets will be installed at the end of the AP1 beamline. A lithium lens[6] may be used to tightly focus the beam on target to very small spots 0.1 mm or less; its greatest disadvantage is that it absorbs 7.5% of the incident proton beam. The upstream magnets will be near the focal point of this lens. The downstream magnets will be located at two currently unoccupied modules between the collection lens and the pulsed magnet, near the focal point of the collection lens. Requirements on the peak deflecting field for expected Main Injector operating conditions are 2.6 kG upstream, and 2.0 kG downstream.

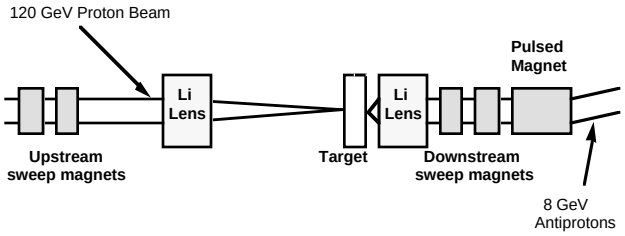

Figure 3. Components in target vault, with locations of sweep magnets shown.

System requirements on timing jitter, field regulation, and field uniformity may be determined from the effective RMS radius x_{RMS} of a displaced beam spot at the target

$$x_{RMS} = \left(\sigma_{bx}^2 + \Delta x^2\right)^{1/2}$$

where σ_{bx} and Δx are the beam spot size and the displacement in a given direction. If we wish to limit the increase in x_{RMS} to less than 10% in all cases, the criterion becomes $\Delta x <$ 0.05mm. The resulting requirements on timing jitter lead to a combined requirement of ± 30 ns. The field uniformity/regulation requirement is $\Delta B/B < \pm 7\%$.

Two current-carrying plates, roughly 3cm wide, with an air gap of 3cm will provide the deflecting magnetic field. A magnetic core surrounding the plates provides a return path for the magnetic field. MARS10 and CASIM calculations of energy deposition by hadron and electromagnetic cascades show significant heating of iron and ferrite magnet cores downstream of the target.[3] Total heating increases linearly with particle flux, and is a strong function of the radius of the magnet core. Steady-state temperature rise of the core is determined by thermal conductivity of the material and the rate at which heat is removed at the surface. Because of its low Curie temperature, a ferrite core design requres the minimization of the use of ferrite at small radii, where the energy deposition is greatest. A laminated iron core does not have the thermal restrictions of a ferrite core, and thus may be closer to the beam path. However very thin .001-inch laminations are required. Investigations are currently underway to determine the feasibility of using a laminated iron core.

Ionization of the air by the particle shower downstream of the target will increase the conductivity of the air between the conductor plates. Electrical losses through the ionized-air path across the gap reduce the Q of the circuit driving the magnet. Estimates based on CASIM calculations predict that the current drain between the plates will be less than 100 A, an acceptable amount. Avalanche ionization of the air does not appear to be a problem, as long as peak electric fields are kept well below breakdown levels, i.e. E<10 kV/cm. The greatest problems are likely to be at the feed points of the strip line to the sweep conductors. Installation of a dummy test module is planned to measure the leakage current between two conductors placed parallel to the beam path at voltages up to 10 kV.

The sweep magnets must be provided with approximately 6 kA at 625-kHz by a power supply located on the floor of the AP0 service building. The current will be supplied through cables over a distance of approximately 10 m into the target vault, and by 2.5 m of strip line through steel shield modules to the magnets at the bottom of the target vault. The inductance of the cable, in series with the sweep magnets, significantly increases the requirements on the power supply. SPICE simulations show that it is possible to supply the

current directly through 16 parallel RG-220 cables with a high-power thyatron switch, but the requirements on the thyratron are severe. Two approaches that reduce the requirements on the power supply are under consideration. In both cases a capacitor is placed at the top of the target vault, connected by a strip line in parallel resonance with the inductance of the sweep magnet, and the resonant circuit is tuned to 625 kHz.

(a) The tuned circuit may be driven by another tuned circuit, coupled in a linear dual-resonant circuit.[1] The circuit components consist of the energy-storage capacitor C_1, the inductance of the pulser and parallel drive cables L_1, and the resonant load, L_2 and C_2 (fig. 4a). The circuit efficiently transfers energy from the primary loop to the secondary loop at the characteristic frequency ω_0 if the following conditions are satisfied:

$$\omega_0^2 L_1 C_1 = \left(\frac{2}{n^2 + m^2} \right)$$

$$\omega_0^2 L_2 C_2 = \left(\frac{m^2 + n^2}{2 n^2 m^2} \right)$$

Here n and m correspond to the resonant mode numbers of the coupled circuit. The mode of greatest interest is $n=2$, $m=3$. The current step-up from the primary to the seconday loop is about 2.6. The energy is supplied to the magnet in 2-3 current reversals, with an initial voltage requirement of approximately 30 kV at a capacitor bank. The necessary current (3-4 kA) can be switched with a hydrogen thyratron.

(b) An alternative approach is pulse compression by saturating inductors. This technique has enjoyed wide acceptance as a passive switching technique for pulsed currents. A two-stage inductive pulse-compression circuit is shown in Fig. 4b. The initially large inductance of a ferrite inductor L_1 allows the relatively slow supplying of energy to an intermediate energy storage capacitor C_1 on a relatively long time scale scale of 10 us. The inductor is designed to saturate when sufficient energy is available to drive the sweep magnet. The process is repeated in the second stage C_2 and L_2. When the inductor L_2 saturates it rapidly discharges C_2 into the resonating capacitor C_3 at the top of the target module, which in turn rings into the sweep magnet L_3. This arrangement allows the use of a simple solid-state SCR-driven power supply, and a simple cable arrangement to deliver the charging current to C_1. Techniques have been demonstrated that control timing jitter to the subnanosecond level.[7]

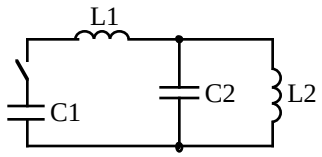

(4a)

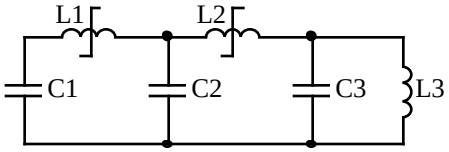

(4b)

Fig. 4. Representative circuits for driving the sweep magnet.

---

*Operated by the Universities Research Association Inc., under contract with the U.S. Department of Energy.

[1] F. M. Bieniosek, A Beam Sweeping System for the Fermilab Antiproton Source, Fermilab-TM-1857 (1993).
[2] S. C. O'Day and F. M. Bieniosek, P-bar Production Measurements at the Fermilab Antiproton Source, Proceedings European Particle Accelerator Conference, 1994.
[3] C. M. Bhat, N. V. Mokhov, Calculation of Beam Sweeping Effect for the Fermilab Antiproton Source, Fermilab-TM-1585 (1989).
[4] S. O'Day, F. Bieniosek, K. Anderson, New Target Results from the FNAL Antiproton Source, Proc. 1993 US Particle Accelerator Conference.
[5] G. I. Silvestrov and A. D. Cherniakin,A Sweeping System for producing Secondary Beams with High Phase Density, IIF-Preprint-84-120 (1984). [translation LA-tr--86-24].
[6] F. M. Bieniosek and K. Anderson, Lithium Lens for Focusing Protons on Target in the Fermilab Antiproton Source, Proc. Particle Accelerator Conf, Washington, 1993.
[7] M. A. Newton and J. A. Watson, Timing and Voltage Control of Magnetic Modulators on ETA II, Proc. 7th IEEE Pulsed Power Conference, Monterey, 1989.